Environmental Challenges 14 (2024) 100866

Contents lists available at ScienceDirect

Environmental Challenges

journal homepage: www.elsevier.com/locate/envc

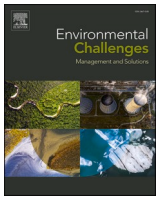

Modeling land use/land cover changes using quad hybrid machine learning model in Bangweulu wetland and surrounding areas, Zambia

Misheck Lesa Chundu *, Kawawa Banda, Chisanga Lyoba, Greyfold Tembo, Henry M. Sichingabula, Imasiku A. Nyambe

Department of Geology, The University of Zambia Integrated Water Resources Management Centre, School of Mines, P.O. Box 32379, Lusaka, Zambia

ARTICLE INFO

Keywords:
Bangweulu
Land use/land cover change
Landsat
Machine learning
Remote sensing
Wetland

ABSTRACT

Wetlands are among the most productive natural ecosystems globally, providing crucial ecosystem services to people. Regrettably, a substantial 64 % –71 % of wetlands have been lost worldwide since 1900, mainly due to changes in land use and land cover (LULC). This issue is not unique to Zambia's Bangweulu Wetland System (BWS), which faces similar challenges. However, there is limited information about the LULC changes in BWS. Furthermore, finding accurate and cost-effective methods to understand LULC dynamics is complicated by the multitude of available techniques for LULC classification. Non-parametric methods like Machine Learning (ML) offer greater accuracy, but different ML models come with distinct strengths and weaknesses. Combining multiple models has the potential to create a more precise LULC classification model. Open-source software like QGIS and spatial data like Landsat also play a significant role in this endeavour. The primary objective of this study was to enhance the accuracy of modeling LULC changes in wetland areas. Six ML models: Support Vector Machine (SVM), Naive Bayes (NB), Decision Tree (DT), Artificial Neural Network (ANN), Random Forest (RF), and K-Nearest Neighbour (KNN) were used for LULC image classification of Landsat 8 (2020 image) and Landsat 5 (1990, 2000, and 2010 images) in QGIS. Four models: SVM, NB, DT, and KNN, performed better than the other models. Consequently, The Quad (4) hybrid model was created by fusing the maps from these four models with the highest performance. Results revealed that the fusion of the four classified maps of the SVM, NB, DT, and KNN (Quad hybrid model) showcased superior performance compared to the individual models with Kappa Index scores of 0.87, 0.72, 0.84 and 0.87 for the years 1990, 2000, 2010 and 2020, respectively. The analysis of the LULC changes from 1990 to 2020 showed a yearly decline of -1.17 %, -1.01 %, and -0.12 % in forest, grassland, and water body coverage, respectively. In contrast, built-up areas and cropland increased at rates of 1.70 % and 2.70 %, respectively. This study underscores the consistent growth of cropland and built-up areas from 1990 to 2020, alongside the reduction of forest cover and grassland. Although the water body experienced a gradual decrease over this period, the decline was minimal. Long-term monitoring will be essential for evaluating the success of interventions, guiding conservation efforts, mitigating negative impacts on the wetland ecosystem, and determining whether the reduction in water bodies is a sustained trend or a short-term phenomenon.

Introduction

Global wetlands are distinct ecosystems in which the water table is usually at or near the land surface or the land is flooded by water (Kumar and Kanaujia, 2018). Ramsar Convention on Wetlands (2018) established that wetlands encompass an approximate area of 12.1 million square kilometers (Km^2) worldwide, of which 54 % are consistently submerged by water, and 46 % are periodically inundated. Wetlands provide a wide range of economic, social, environmental, and cultural benefits that are collectively referred to as ecosystem services (Costanza et al., 1997). Zedler and Kercher (2005) emphasized that despite covering merely 1.5 % of the Earth's surface, wetland ecosystems play a crucial role in providing approximately 40 % of global ecosystem services. These services include (1) provisioning services (food, fresh water supply, fiber, and fuel), (2) regulation service (influence on air quality, climate regulation, regulation of water flows, erosion prevention) (3) habitat/support services (gene pool protection, lifecycle maintenance) (4) cultural services (recreation/tourism, spiritual, aesthetic) (Zedler

* Corresponding author.
E-mail address: misheckchundu@gmail.com (M.L. Chundu).

https://doi.org/10.1016/j.envc.2024.100866
Received 31 October 2023; Received in revised form 4 February 2024; Accepted 5 February 2024
Available online 7 February 2024

and Kercher, 2005; De Araujo Barbosa et al., 2015).

African wetlands play a crucial role in providing essential ecosystem services that directly support the livelihoods of numerous rural communities (Simaika et al., 2021). Despite the multitude of benefits that wetlands provide, they face significant threats due to land use/land cover (LULC) changes which include the establishment of settlements, expansion of agricultural activities, and various other human-related actions (Winton et al., 2021) which are far more prevalent than natural phenomena like storms, landslides and earthquake (Galatowitsch, 2018).

Banda et al. (2023) reported that LULC changes are among the many drivers that profoundly impact ecosystem services by altering the natural functions of wetlands. Davidson (2014) also reported that 64–71 % of wetlands have been lost worldwide since 1900 due to anthropogenic factors. Zhang et al. (2021) added that the anthropogenic factors such as urban growth, has led to wetlands being drained, filled, or altered, resulting in the loss of valuable wildlife habitats (FAO, 2017; Xu et al., 2019). Furthermore, 80 % of global wastewater enters wetlands, posing health risks (FAO, 2017; Xu et al., 2019). Xu et al. (2019) also added that these factors actually threaten the health and survival of the major wetlands. Therefore, Maitima et al. (2010) concluded that LULC changes can have detrimental effects such as modifying the wetlands' ability to control floods, disrupting sediment and nutrient transport, compromising aquatic biodiversity, obstructing the migration routes of aquatic organisms, increasing soil salinity, making wetlands more susceptible to erosion, and disturbing the connectivity of river systems.

Zambia has eight wetlands designated as wetlands of international importance, which are spread throughout seven river basins (Ngoma et al., 2017; Ren et al., 2021). These wetlands, especially the Bangweulu (meaning "water meets the sky") Wetland System (BWS), are critical for biodiversity and environmental services. The BWS is one of Zambia's most highly prioritised sub-catchments for protection (Lehner et al., 2021). However, the BWS faces the threats of LULC changes such as excessive exploitation of ecosystem services by local populations, unsustainable development and fishing practices, deforestation, and agricultural expansion (Kamweneshe et al., 2003; Zambia Wildlife Authority, 2006; Zambia Environment Outlook Report 4, 2017). Despite these threats, literature is inadequate on the LULC changes related to the BWS and its surrounding areas. The surrounding areas consist of regions where streams flow into the BWS (Kamweneshe et al., 2003; Zambia Wildlife Authority, 2006). This knowledge gap complicates understanding and effectively managing the dynamic nature of the BWS.

Timely and accurate detection of changes in the BWS surface features is critical for wetland conservation, sustainable development, and water resource management as well as understanding the interactions between human and natural phenomena (Lu et al., 2004; Wulder et al., 2019). Recent advances in remote sensing tools and techniques enable researchers to detect and monitor such changes at a large scale, as remote sensing data like Landsat data are used as the primary source for change detection (Hemati et al., 2021). The Landsat data are crucial for environmental and ecological monitoring as they provide early baseline data for change detection in areas with valuable ecosystems (Wulder et al., 2019; Hemati et al., 2021).

It should be noted that for several decades, the statistical approach, specifically parametric methods, has served as the conventional method for fitting models in LULC classification. This approach operates under the assumption that the data is generated using a stochastic data model (Loussaief and Abdelkrim, 2017). The challenge with this approach is that they work with a pattern that can be statistically well analysed but can not be predicted precisely. As a result, statistical data model conclusions are about the model's mechanism rather than nature's mechanism; if the model is a poor emulator of nature, the conclusion may be incorrect (Breiman, 2001a; Loussaief and Abdelkrim, 2017). Furthermore, statistical models in spatial LULC analysis are problematic because they assume that data is statistically independent and uniformly distributed. However, spatial LULC data are highly heterogeneous and tend to be dependent, a phenomenon known as spatial autocorrelation (Charif et al., 2012).

Machine Learning (ML) is a field of artificial intelligence (AI) and computer science that is based on the idea that systems can learn from data and algorithms modeling culture to mimic how humans learn, identify patterns, and make decisions (Breiman, 2001a; Chollet, 2017). The use of ML models in this research was primarily motivated by the models' universal approximation capabilities and high performance in a wide range of scientific fields (Charif et al., 2012). ML employs algorithmic models that treat the data mechanism as unknown, complex, and highly heterogeneous. In addition, algorithmic modeling can be used on large complex data sets as well as on smaller data sets as a more accurate and informative alternative to statistical data modeling (Breiman, 2001a; Loussaief and Abdelkrim, 2017).

ML algorithms can be used to predict how ecosystems respond to changes in environmental variables by detecting nonlinear empirical relationships between variables based on a set of representative data sets (Antunes et al., 2021; Sadiq et al., 2019). Hence, ML algorithms prove to be valuable tools for modeling complicated ecosystems like wetlands. Their advantages encompass operational simplicity, reliability in handling nonlinearity, robustness, and the ability to handle noisy data (Kang et al., 2012; Antunes et al., 2021). There are several classification algorithms used in ML which include: (1) Artificial Neural Networks (ANNs), (2) Naïve Bayes (NB), (3) Support Vector Machines (SVM), (4) Decision Tree (DT), (5) Random Forest (RF), and (6) K-Nearest Neighbour (KNN) algorithms, among others.

ML models, being diverse in nature, possess unique sets of strengths and weaknesses that set them apart from one another. These distinctions arise due to differences in algorithmic approaches, training data requirements, interpretability, generalisation capabilities, computational efficiency, methods, time and space, and robustness to noise (Cutler et al., 2012; Qiu et al., 2015; Chen et al., 2020). Therefore, experimentation and evaluation of different ML models on the specific task are crucial to determine the best model that is capable of achieving reliable accuracy (Maxwell et al., 2018; Camargo et al., 2019; Talukdar et al., 2020). The multiple best models can then be integrated into a hybrid model which would allow for the creation of a more powerful and accurate model by leveraging the diverse strengths and weaknesses of different models (Polikar, 2006; Rokach, 2010).

The use of machine learning approaches such as SVM, DT, AAN, RF, NB, and KNN in Africa has shown success in improving LULC classification performance (Boateng et al., 2020; Mahmoud et al., 2023; Yuh et al., 2023). However, these methods often require significant image pre-processing, especially with coarse-resolution images, to reduce uncertainties in LULC classifications. Furthermore, there has been limited application of these approaches to effective monitoring of changes in LULC within wetland areas across Africa (Yuh et al., 2023), where coarse-resolution satellite images are frequently the only available option. Existing studies have generally relied on applying only a single method (Gxokwe et al., 2023; Thamaga et al., 2022; Yuh et al., 2023), which can increase classification uncertainties relative to the use of an ensemble approach.

The contributions of this study to literature include the use of six distinct ML models (SVM, NB, DT, ANN, RF, and KNN) for the LULC classification of Landsat data. In addition, the paper presents a novel method for achieving a more accurate LULC classification: it builds a Quad hybrid model by combining the maps from the four top-performing ML models (SVM, NB, DT, and KNN). This kind of classification approach was also recommended by Ouma et al. (2022) who concluded that this strategy could perform better than individual models. Furthermore, the research offers valuable perspectives on LULC changes in the study area, with possible implications for policy and management choices, these contributions deepen our understanding of LULC dynamics and wetland protection.

The main objective of this study was to enhance the accuracy of modeling LULC changes in wetland areas, encompassing the past and the

present (1990 to 2020). This could facilitate informed decision-making processes for wetland management and conservation, particularly in developing nations. The following were the specific objectives: (1) to identify the best performing ML models in LULC classification, (2) to develop a superiorly hybrid ML model for modeling the past and present LULC changes (from 1990 to 2020), and (3) to determine the extent of LULC changes between 1990 and 2020. In this research, it was hypothesised that integrating multiple machine learning models into a hybrid model could result in improved performance compared to individual models alone.

Materials and methods

Study area description

The BWS, located in Zambia's upper Congo River basin, covers an area of about 30,000 km^2, with over 11,900 km^2 of seasonally flooded plains and permanent swamps. The system is characterised by seasonal flooding, which impacts the local economy and environment. The climate is divided into three distinct seasons: a cool dry season from April to August, a hot dry season from August to October, and a warm wet season from November to April. The wetland is fed by 17 major rivers from a catchment area of 190,000 km^2 but is only drained by one river, the Luapula River (Kamweneshe et al., 2003).

The BWS has five vegetation zones: upper mainland woodland, fringing open woodlands, termitaria and fringing grasslands, seasonal floodplain, and permanent swamp. Upper mainland woodlands consist of miombo trees and grassy understory. Termitaria zones have dense tree and shrub growth due to termite mounds. Open waters have submerged macrophytes, while flooded areas near papyrus swamps are dominated by grass. Deep-water floodplains have semi-floating grasses and sedges, including permanently inundated sections (Fanshawe, 1971; Storrs, 1995; Zambia Wildlife Authority, 2006).

The area is home to both endemic species like black lechwe and numerous bird species, as well as a human population of over 50,000 living within the wetland (Kamweneshe et al., 2003; Zambia Wildlife Authority, 2006). The study area (Fig. 1) is a sub-catchment of the Luapula River Basin with an estimated area of 75,158.143 Km^2 which covers the Bangweulu Wetland (30,000 km^2) and the surrounding areas (45,158.143 Km^2).

Methods for data collection and analysis

Field and spatial data

Several studies highlight the significance of having a sufficient number of training samples and the general pattern of enhanced classification accuracy as the sample size increases. However, these studies do not explicitly offer specific conclusions or optimal recommendations for sample sizes in LULC classification tasks as the appropriate sample size is determined by various factors, including the type of model used, predictor variables, LULC class definition, as well as the size and spatial characteristics of the study area (Ma et al., 2017; Hernandez et al., 2020; Mohammadpour et al., 2022).

Ramezan et al. (2021) investigated the impact of sample size on various machine-learning models. The results revealed a minimal decrease of 1 % in overall accuracy when the training sample size ranged from 315 to 10,000 samples. Moraes et al. (2021) also conducted a study on the impact of sample size (50 to 6000 samples) in LULC classification using Random Forest and found that 2000 samples achieved the highest accuracy (73.7 %), while 6000 samples yielded the lowest accuracy (71.5 %). Despite a drastic reduction in training sample units, there was only a 2 % accuracy variation, indicating consistent classification accuracy performance. Furthermore, different studies have used different numbers of training samples. For example, Kulkarni & Lowe (2016) trained the Random Forest model using the dataset of 600 samples and achieved an overall accuracy of 96 %. Laban et al. (2019) utilized 708 training and validation samples for various machine learning LULC classifications, resulting in an overall accuracy rate of 92.7 %, 92 %, 92.1 %, and 94.4 % for the RF, K-NN, ANN, and SVM algorithms, respectively.

In view of the above, this research considered the use of cost-effective methods by using minimum training samples that could still yield desirable performance for modeling LULC changes. Therefore, we employed purposive sampling, wherein the researcher selected elements to be included in the sample based on their relevance to the study topic and the prevailing conditions in the field as described by Etikan (2016).

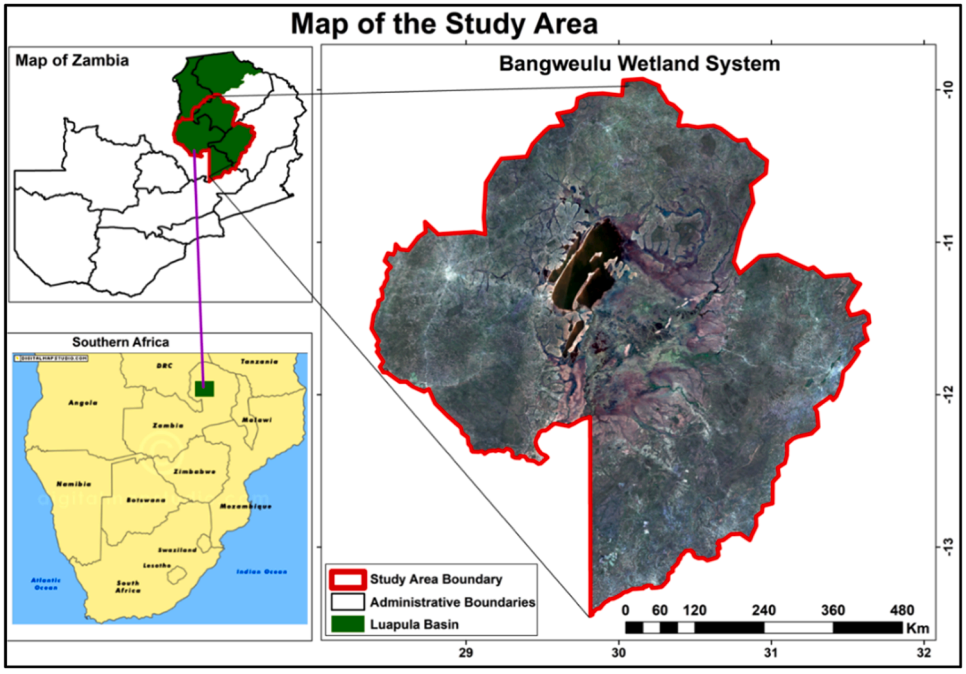

Fig. 1. The location of the Bangweulu Wetland System and the surrounding areas in Zambia. The red boundary shows the exact extent of the study area, which is a sub-catchment of the Luapula Basin.

We used a combination of field surveys conducted between October to December 2022 and March to April 2023, and a visual inspection of very-high-resolution images available on Google Earth Pro-to collect training and validation data for the 2020 image. This approach allowed us to create a total of 800 polygons for training and validation purposes.

During the field investigations, 315 geometry points were collected from accessible areas representing various LULC categories, namely built-up areas (including roads, settlements, and barren land), grasslands (all grass types and open shrubs), forests (encompassing thick shrubs and wooded regions), croplands, and water bodies. The geometry points were superimposed on the 2020 Landsat image and 315 polygons were created based on the location of geometry points.

Additionally, the 315 training and validation polygons were supplemented with 485 other polygons. This supplemental dataset of polygons was created through visual inspection of high-resolution images obtained from Google Earth Pro, which represented various LULC classes and served as an additional source of information for training and validating the models. To obtain the coordinates and attribute information of LULC, we primarily relied on a handheld global positioning system (GPS). We also relied on a visual inspection of the Google Earth pro time series, the Landsat images, and the researcher's expertise to create the training and validating dataset of polygons for 1990, 2000, and 2010 images.

Data partitioning

The dataset containing 800 polygons was partitioned into five segments based on the following percentages: 60 %, 10 %, 10 %, 10 %, and 10 %, resulting in 480, 80, 80, 80, and 80 polygons, respectively. The 60 % portion and one of the 10 % portions were allocated for model development and validation, respectively. The remaining three 10 % portions were set aside specifically for conducting triple post-classification accuracy assessment, as illustrated in Fig. 3. A triple cross-validation was used to enhance the reliability of the model's LULC classification and the averaged results obtained through cross-validation were reported as the main performance of the model. Reporting averaged metrics enhances transparency and facilitates fair comparisons among different models. These results provide a more robust and representative evaluation, accounting for the variability of the data and offering a reliable estimate of the model's performance on unseen samples (Basheer et al., 2022; Hosseiny et al., 2022). Fig. 2 shows the distribution of training and validation polygons in the study area.

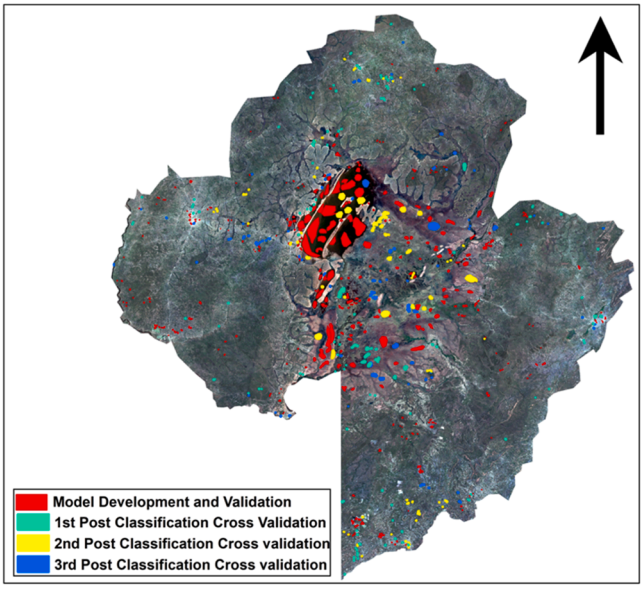

Fig. 2. Distribution of the model development, validation, and post -classification cross-validation polygons for 2020 Landsat image based on field data and Google Earth Pro. For the red polygons (560 polygons), the algorithms picked at random 480 and 80 polygons for model development and validation, respectively.

Spatial data

Annual average conditions of preprocessed images of Landsat 5 (1990, 2000, and 2010 images) and Landsat 8 (2020 image) with four bands (near-infrared, red, green, and blue) of the Bangweulu Wetland and the surrounding areas were downloaded from Climate Engine (https://app.climateengine.com/climateEngine). The annual average conditions of pre-processed images are single average images generated by the Climate Engine by combining several input images from January to December (Huntington et al., 2017). The downloaded images were classified using various machine learning algorithms (ANN, NB, SVM, DT, RF, and KNN algorithms) through the Orfeo Toolbox in QGIS 3.28.5.

Model development and accuracy assessment

Various algorithms, namely ANN, NB, SVM, DT, RF, and KNN were used for model development. The models were created using a total of 480 reference polygons as training data samples, and an additional 80 reference polygons were reserved for evaluating the accuracy of the models. This process is visually depicted in Fig. 3. Among the developed models, those that demonstrated exceptional performance, surpassing the others with a Kappa Index (KI) exceeding 0.60 were selected for further analysis based on Table 2.

Model development set parameters

The parameters for various algorithms used in the model development were established by taking into consideration the guidelines of various scholars as well as fine-tuning their specific parameters through trial and error thereby ensuring that each model achieved the best possible performance. For RF, the following number of trees were used for fine turning 10, 50, 100, and 150. However, different numbers of trees did not provide sufficient influence on the classification results. This observation was expected as it has already been reported by other scholars (Guan et al., 2013; Belgiu and Drăgu, 2016). Therefore, the default setting value (100) of the Orfeo Toolbox in QGIS was used. Similarly, the default value (32) of K was also used for KNN. For SVM and DT, the parameters used were based on the findings of various scholars (Gholami and Fakhari, 2017; Abidi et al., 2020; Ramezan et al., 2021). The parameters used are presented in Table 1.

Image classification and triple cross validation

The selected models were employed to classify images from the years 1990, 2000, 2010, and 2020. The resulting classified maps underwent triple cross-validation using three distinct sets of 80 reference polygons. Cross-validation is a widely used procedure for validation of the LULC classification models. One subset of the dataset is used for model training, and another subset is used for validation. This is done for multiple (k-fold) times, and the results are eventually averaged to get a more robust assessment of the model's performance (Hayes et al., 2014). In this research post classification model validation was done using three different datasets. Therefore, Triple (3-fold) cross-validation was the name given to the three-step cross-validation process, and the averaged Kappa Index (KI) was used to select a more accurate model's performance estimate. This accuracy evaluation process was referred to as post-classification triple validation. The average value of the KI obtained from this assessment was used to identify the models with the highest performance. Models that had a triple cross-validation KI average below 0.60 were excluded, while those with a KI exceeding 0.6 were selected for further analysis, this was based on Table 2.

Fusion of classified maps and triple cross validation

The classified maps from the best-selected models were fused to create a hybrid map representing the LULC classes for the years 1990, 2000, 2010, and 2020. The resulting hybrid maps also underwent triple

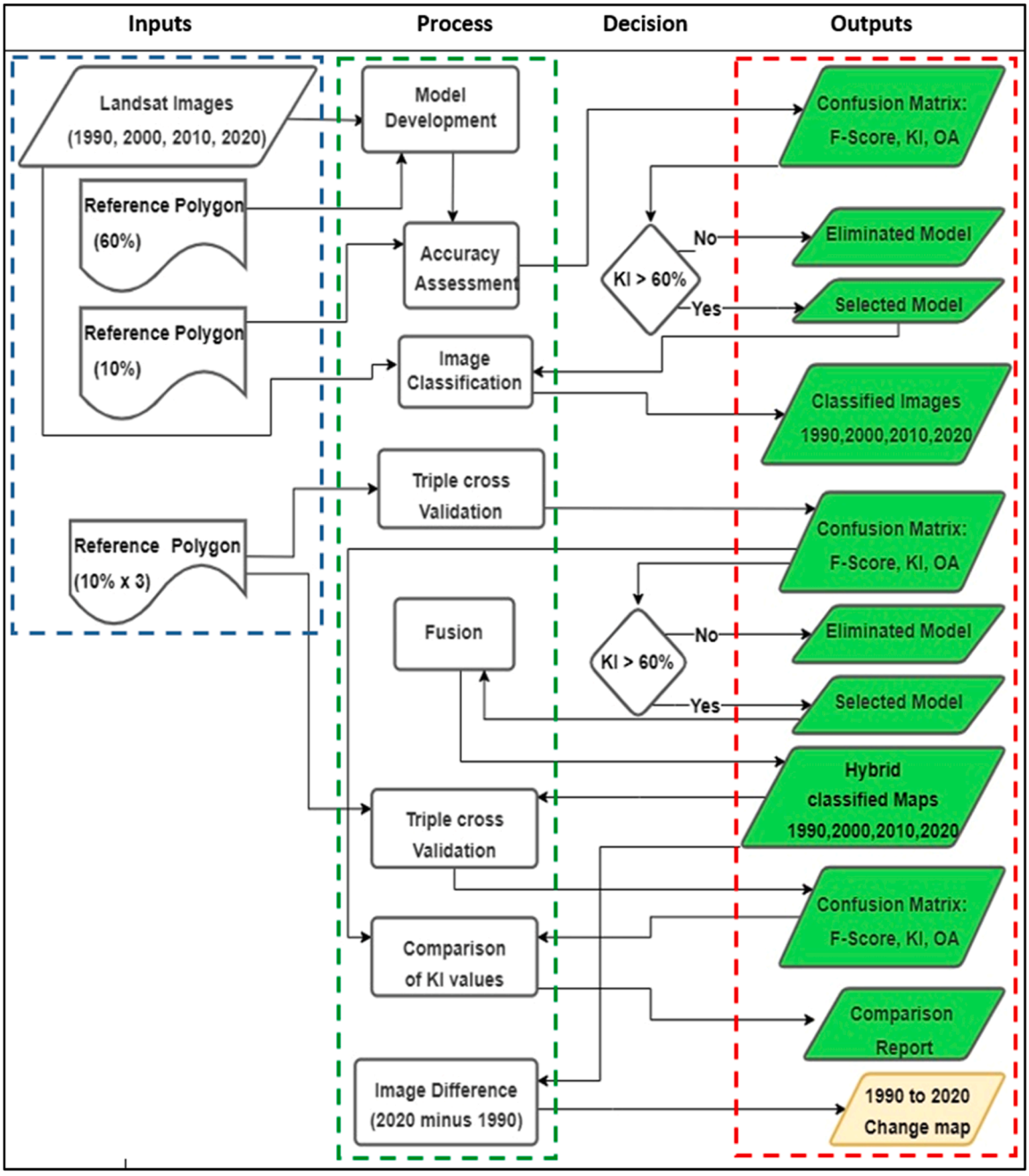

Fig. 3. A summary of the research materials and method.

cross-validation using the same three sets of 80 reference polygons. This was done to compare the accuracy of the hybrid classified maps with the individual models classified maps (refer to Figs. 3 and 6).

Area changes between 1990 and 2020

The change map was realised by finding the difference between the 2020 and 1990 hybrid maps. In addition, the annual rates of LULC change (ARC) as illustrated in Eq. (1), were calculated using the following formula:

$$\mathrm{ARC} = ((\mathrm{LULC\_end} - \mathrm{LULC\_start}) / \mathrm{LULC\_start}) * 100/(\mathrm{number\ of\ years}). \quad (1)$$

Where:

- LULC_start is the value of LULC at the start of the period.
- LULC_end is the value of LULC at the end of the period.
- Number of years: years between the start and end of the period.

Metrics for accuracy assessment

The metrics employed to evaluate the accuracy of the models' performances were the Kappa Index (KI) (Eq. (2)), Overall Accuracy (OA) (Eq. (3)), and F-score (Eq. (4)) of the LULC classes.

Kappa index

The Kappa index (KI) was calculated as shown in Eq. (2) (Alshari and Gawali, 2022; Zhang et al., 2021).

$$\mathrm{KI} = \frac{(\mathrm{Po} - \mathrm{Pe})}{(1 - \mathrm{Pe})} \quad (2)$$

Where:

Table 1
The specific input parameter values for different models.

	Model		Parameters		
1	SVM	Kernel type	Cost	Gamma	SVM type
		RBF	4	0.033	CSVC
2	DT	Maximum depth of Trees	Minimum number of samples in each node	Random seed	
		10	10	0	
3	RF	Number of trees in forest	Random seed	–	–
		100	0		
4	KNN	Number of Neighbours	–	–	
		32			
5	NB	–	–	–	–

*Assumption: the parameters used in Table 1 were assumed to be optimal.
RBF: Radial Basis Function kernel, CSVC: Complex-valued Support Vector Classifier.
ANN: is missing from the list because it could not be executed (check Section 3.1).

Table 2
KI interpretation.

Value of Kappa Index	Level of Agreement
−1 - 0.20	None
0.21 - 0.39	Minimal
o.40 - 0.59	Weak
0.60 - 0.79	Moderate
0.80 - 0.90	Strong
Above 0.90	Almost Perfect

Adapted from Landis & Koch (1977) and McHugh (2012).

- P_O is the proportion of agreement between classified LULC classes and reference datasets.
- Pe is the sum of the product of the row and column marginal proportions for each category, divided by the total number of observations squared.

KI value ranges from −1 to 1, Where:

- KI = 1 indicates perfect agreement.
- KI = 0 indicates agreement that is no better than chance.
- KI < 0 indicates agreement worse than chance.

Overall Accuracy

The Overall Accuracy (OA) as illustrated in Eq. (3), provides a measure of how accurately the model assigns the correct class to each pixel or sample. The equation sums up the correctly classified samples (both positive and negative, i.e., the sum of the values on the major diagonal) and divides it by the total number of samples in the dataset (Congalton, 2001).

$$OA = \frac{(TP + TN)}{(TP + TN + FP + FN)} \quad (3)$$

Where:

- TP (True Positive) represents the number of correctly classified pixels or samples belonging to the positive class.
- TN (True Negative) represents the number of correctly classified pixels or samples belonging to the negative class.
- FP (False Positive) represents the number of incorrectly classified pixels or samples that were wrongly assigned to the positive class.
- FN (False Negative) represents the number of incorrectly classified pixels or samples that were wrongly assigned to the negative class.
- OA ranges from 0 to 1, where 1 indicates perfect classification accuracy and 0 indicates no accuracy at all.

F-Score

The F-score (Eq. (4)), also referred to as the F1 score or F-measure serves as a performance metric for evaluating Machine Learning models. It combines precision and recall into a single metric by calculating their harmonic mean. This harmonic mean places more emphasis on lower values, making it a suitable metric when precision and recall need to be balanced. Precision measures the accuracy of positive predictions, while recall quantifies the model's ability to identify all positive samples. The F-score, ranges from 0 to 1, with higher values indicating better accuracy (Dalianis, 2018).

$$F - score = 2 * \left(\frac{Precision * Recall}{Precision + Recall}\right) \quad (4)$$

However, the KI in this research was the primary metric used in the elimination of underperforming models. Any model with KI less than 0.60 was eliminated. This was based on (Landis and Koch, 1977; McHugh, 2012) as depicted in Table 2.

Fig. 3 serves as a comprehensive visual representation of all the different materials and methods we used in this research and how they were combined at different stages.

Results

Model development accuracy assessment

The findings indicated that the KNN algorithm exhibited the highest accuracy in model development for the 1990, 2000, and 2020 images, yielding KI values of 0.958, 0.918, and 0.969, respectively. However, for the 2010 images, the SVM algorithm displayed the highest model development accuracy with a KI of 0.964 (refer to Fig. 4). Generally, all the algorithms showed consistent and robust performance across different classes of LULC, with F-scores ranging from 0.764 to 1 (Table 3). The highest accuracy was achieved in identifying water bodies, with an F-score of over 99 % (Table 3), indicating near-perfect classification results for this specific class. This evaluation suggests that all the algorithms are effective in LULC classification, especially for water bodies, which is critical for various environmental and geospatial applications. ANN model which could not be executed due to a bug in the latest version of QGIS Desktop 3.28.5, therefore, was excluded at this stage and was not considered in the subsequent analysis.

LULC classification and triple cross-validation (Post classification accuracy)

The selected models (SVM, NB, DT, RF, and KNN) were used to create LULC maps for the study area. To evaluate the accuracy of the classified maps, a triple cross-validation approach was utilised, incorporating 80 samples organised in triplets (refer to Fig. 3 above). Upon assessing the results, it was observed that all models generally exhibited poor performance in classifying cropland in 1990 and 2000, indicated by F-scores ranging from 0.06 to 0.42 (Table 4). This poor performance was attributed to the low quality of the 1990 and 2000 Landsat 5 images which had sparkles.

The RF model performed well on the training data but it could not generalise well to the new, unseen data model for the classification of 1990 and 2000 images where it failed to meet the KI threshold of 0.60 (refer to Fig. 5 and Table 2). The primary factor contributing to the RF model's low performance was its misclassification of the built-up, grassland, and cropland classes of the 1990 image, with corresponding F-scores of 0.070, 0.011, and 0.264, respectively (refer to Table 4). Furthermore, the model struggled in classifying forest cover and cropland in 2000 images, achieving F-scores of 0.529 and 0.281, respectively

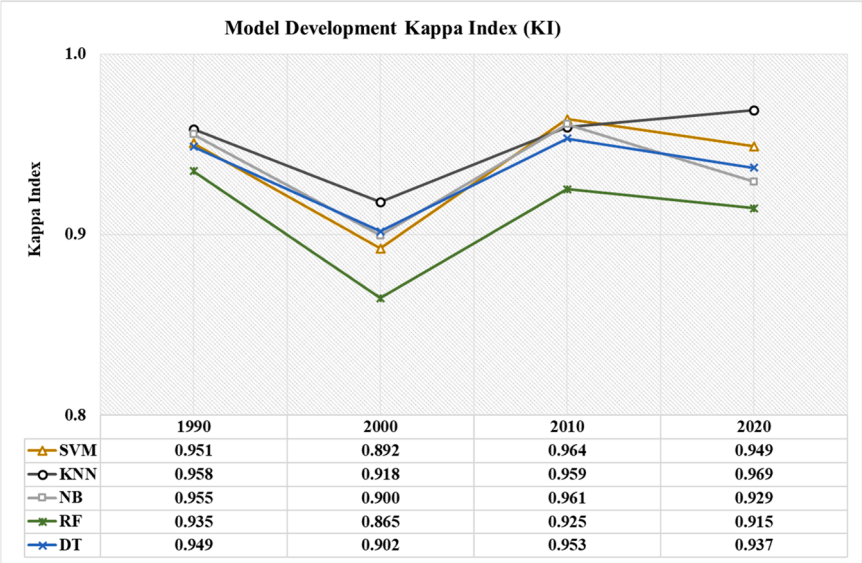

Fig. 4. Model development Kappa Index of different machine learning models.

Table 3
Model development F-Score of different machine learning models.

	Model Development F-Score of Class							Model Development F-Score of Class				
	Model	F Forest	Built-up	Grassland	Water	Cropland		Model	F Forest	Built-up	Grassland	Water	Cropland
	NB	0.969	0.979	0.921	1	0.951		NB	0.912	0.989	0.857	0.998	0.842
	DT	0.964	0.986	0.905	1	0.941		DT	0.911	0.990	0.846	1	0.858
1990	KNN	0.970	0.988	0.920	1	0.953	2000	KNN	0.928	0.990	0.876	1	0.877
	RF	0.959	0.987	0.876	1	0.917		RF	0.871	0.990	0.764	1	0.826
	SVM	0.961	0.988	0.905	1	0.947		SVM	0.912	0.991	0.829	1	0.837
		Model Development F-Score of Class							Model Development F-Score of Class				
	Model	F Forest	Built-up	Grassland	Water	Cropland		Model	F Forest	Built-up	Grassland	Water	Cropland
	NB	0.978	0.980	0.949	1	0.937		NB	0.982	0.978	0.898	0.995	0.865
	DT	0.976	0.986	0.931	1	0.921		DT	0.994	0.985	0.891	0.996	0.883
2010	KNN	0.976	0.989	0.940	1	0.931	2020	KNN	0.984	0.990	0.959	1	0.942
	RF	0.966	0.988	0.868	1	0.880		RF	0.995	0.986	0.831	0.999	0.844
	SVM	0.975	0.988	0.948	1	0.944		SVM	0.996	0.986	0.912	0.995	0.907

(refer to Table 4). The observed low F-score by the RF model in built-up, cropland, and grassland classification could potentially be attributed to the study area's unique characteristics. Specifically, the majority of the study area consists of remote regions characterised by thatched mud houses, which are surrounded by agricultural fields, bare land, fallow land, and grassland. These LULC types may share similarities in terms of color, texture, and shape, making it challenging to accurately distinguish between cropland, grassland, and built-up areas (Lasanta and Vicente-Serrano, 2012; Wambugu et al., 2021). Consequently, the RF model was excluded at this stage and not considered for further analysis. The SVM, NB, DT, and KNN models exhibited strong performance with KI values ranging from 0.60 to 0.86. As a result, these models were selected for subsequent evaluation (refer to Fig. 5 and Table 4).

Fusion of selected models' maps and triple cross-validation

The classified maps generated by the remaining four selected models (SVM, NB, DT, and KNN) were fused to produce a single hybrid map for each of the years 1990, 2000, 2010, and 2020. This fusion of the classified maps from the four models is referred to as the Quad (4) hybrid model. To evaluate the accuracy of the LULC maps derived from the Quad hybrid model, a triple cross-validation approach was employed, using the same 80 samples organised in triplets as described earlier (Fig. 3 above).

It was observed that the Quad hybrid model developed as a superior machine learning model by combining the classified maps from SVM, NB, DT, and KNN, exhibited superior performance compared to using individual models alone. This was evident from the F-scores, OA, and KI values obtained across all classes (Fig. 6 and Table 4). Specifically, for the years 1990, 2000, 2010, and 2020, the Quad hybrid model achieved KI values of 0.87, 0.72, 0.84, and 0.87, respectively (Fig. 6). These values indicated a higher level of accuracy and reliability in the classification results compared to using the individual models separately.

LULC maps between 1990 and 2020

The Quad hybrid model was employed to produce hybrid maps (from the years 1990, 2000, 2010, and 2020) with five distinct LULC classes, namely forests, built-up areas, grasslands, bodies of water, and cropland. The changes in LULC over the period from 1990 to 2020 were documented and analysed. The findings revealed a general upward trend in land use activities, particularly in the regions encompassing the islands in the wetland and the surrounding wetland areas (Fig. 7 and Table 5).

Bangweulu wetland and the surrounding area change map from 1990 to 2020

The creation of LULC change maps for the period between 1990 and

Table 4
F-Scores, Overall Accuracy (OA) and Kappa Index (KI) of different machine learning models.

		Average of triple Cross Validation F-Score of Class								Average of triple Cross Validation F-Score of Class							
	Model	Forest	Built- up	Grassland	Water	Cropland	OA	KI		Forest	Built- up	Grassland	Water	Cropland	OA	KI
1990	NB	0.916	0.952	0.963	1	0.243	0.941	0.857	2000	0.782	0.965	0.919	0.983	0.364	0.876	0.680
	DT	0.884	0.990	0.950	1	0.193	0.924	0.826		0.703	0.991	0.899	1	0.345	0.850	0.638
	RF	0.874	0.070	0.011	1	0.264	0.239	0.177		0.529	0.974	0.803	1	0.281	0.738	0.480
	KNN	0.855	0.966	0.933	1	0.157	0.902	0.783		0.673	0.980	0.925	1	0.401	0.883	0.693
	SVM	0.735	0.690	0.949	1	0.096	0.913	0.800		0.781	0.901	0.872	1	0.299	0.818	0.601
	Quad	0.925	0.984	0.962	1	0.329	0.946	0.874		0.783	0.977	0.925	0.998	0.420	0.888	0.717
		Average of triple Cross Validation F-Score of Class								Average of triple Cross Validation F-Score of Class							
		Forest	Built- up	Grassland	Water	Cropland	OA	KI		Forest	Built- up	Grassland	Water	Cropland	OA	KI
2010	NB	0.712	0.924	0.967	1	0.862	0.943	0.816	2020	0.908	0.895	0.957	0.954	0.480	0.921	0.829
	DT	0.584	0.915	0.938	1	0.675	0.900	0.722		0.800	0.873	0.939	0.962	0.440	0.893	0.778
	RF	0.650	0.965	0.929	1	0.568	0.887	0.688		0.887	0.884	0.852	0.964	0.244	0.793	0.628
	KNN	0.650	0.965	0.929	1	0.568	0.887	0.688		0.883	0.892	0.942	1	0.418	0.899	0.789
	SVM	0.674	0.924	0.950	1	0.786	0.919	0.767		0.899	0.877	0.944	0.965	0.440	0.904	0.798
	Quad	0.718	0.969	0.970	1	0.906	0.949	0.835		0.910	0.897	0.971	0.971	0.567	0.941	0.870

2020 involved a comparison of classified images from those respective years. This pixel-by-pixel analysis enabled the identification of areas where changes in LULC had taken place. The resulting change map provided a visual representation of the alterations in the distribution and composition of different LULC classes from 1990 to 2020 (Fig. 7A to D). The LULC change map (Fig. 7E) serves as a valuable tool for comprehending and monitoring environmental changes and evaluating the impacts of human activities. It highlights notable transitions that occurred during the studied period, such as the conversion of more than 13,119 Km2 of forest cover and 4821.3 Km2 of grassland area into cropland (Fig. 8). These findings provide valuable insights into the dynamic nature of the landscape and can aid in making informed decisions regarding land use and resource management.

The geographical extent and the corresponding percentage coverage values for the LULC maps depicted in Fig. 7 are detailed comprehensively in Table 5.

Trend analysis of different LULC classes (1990 – 2020)

The analysis of trend curves for various LULC classes revealed noticeable deviations, encompassing both gains and losses. A comprehensive summary of the LULC variations within the study area from 1990 to 2020, can be found in Table 6, as well as Figs. 8, 9 and 10. Generally, the findings indicated a decline in forest cover, water bodies, and grasslands, while there was an increase in cropland and built-up areas between 1990 and 2020. Forest cover remained relatively stable between 1990 and 2010 but experienced a significant decrease thereafter until 2020. The grassland exhibited a sharp reduction in size between 1990 and 2010, followed by a period of stabilization. Water bodies also demonstrated a notable decrease from 1990 to 2010, but a positive change was observed between 2010 and 2020 as shown in Figs. 9 and 10.

Built-up area change analysis

The built-up area in the Bangweulu Wetland and its surrounding areas has undergone a significant increase between 1990 and 2020, as observed from the assessment of changes in the classified maps. Specifically, the built-up area has expanded from 428.89 Km^2 to 873.29 Km^2, representing a growth of over 50 % (Figs. 9 and 10, and Tables 6). The period from 1990 to 2000 witnessed the most substantial rise in the built-up area, with an increase of more than 40 %, this kind of trend was observed by other studies (Kafy et al., 2020, 2022; Taiwo et al., 2023). This was followed by the period from 2010 to 2020, which recorded a growth of 23.44 %. The period from 2000 to 2010 experienced a comparatively lower increase of 17.27 % (Fig. 10 and Table 6). The annual rate of change (ARC) of the built-up areas from 1990 to 2020 was 1.7 % (Table 6).

Forest cover change analysis

The forest cover in the Bangweulu Wetland and its surrounding areas exhibited a significant decline between 1990 and 2020. The average ARC for this period was calculated at −1.17 %, (Table 6) indicating a notable decrease in forest cover over time. This type of trend was also observed by other studies (Kafy et al., 2022; Rahaman et al., 2022). Specifically, the forest cover decreased from 43,185.75 Km2 to 31, 973.485 Km2, which corresponds to a decline of 35.07 % between 1990 and 2020 (Figs. 9 and 10, and Table 6). The most substantial decrease in forest cover occurred during the decade from 2010 to 2020, with a reduction of 23.50 %. This was followed by the period from 1990 to 2000, which witnessed a decrease of 2.85 %. Comparatively, the smallest decrease in forest cover was observed during the period from 2000 to 2010, with a decline of only 0.38 % (Fig. 10 and Table 6).

Cropland area change analysis

The cropland areas in the Bangweulu Wetland and its surrounding areas exhibited a remarkable increase from 3925.11 Km^2 to 20,607.57

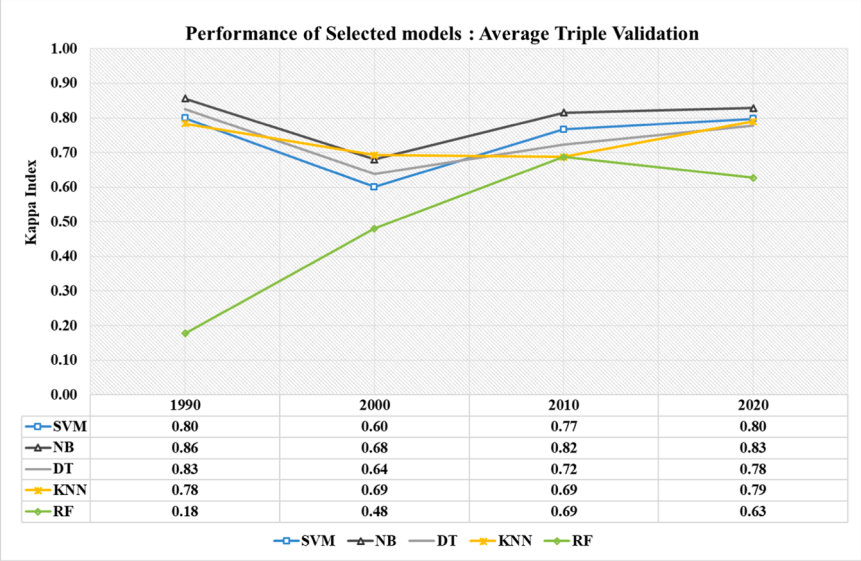

Fig. 5. Post-classification accuracy assessment of the performance of different machine learning models.

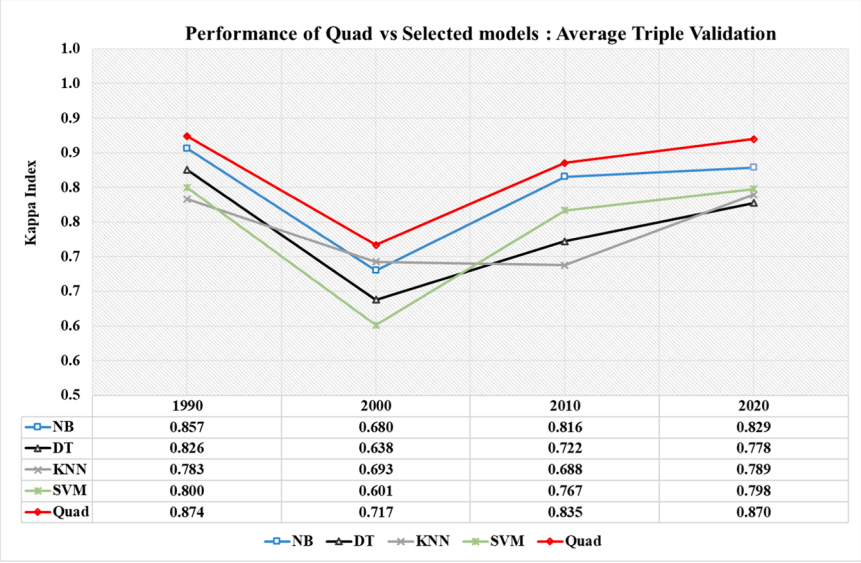

Fig. 6. Quad hybrid model performance compared to the four best-selected models.

Km^2, representing a growth of 80.95 % between 1990 and 2020 (Figs. 9 and 10, and Table 6). A similar trend was also observed by Gxokwe et al. (2023). The average ARC for this period was calculated at 2.7 % (Table 6), indicating a consistent upward trend in cropland expansion. The most substantial increase in the area under crop production occurred between 2010 and 2020, with a notable rise of 83.28 %. This was followed by a 70.28 % increase between 2000 and 2010 and a 68.23 % increase between 1990 and 2000 (Fig. 10 and Table 6).

Water body change analysis

This particular LULC class holds significant importance within the study area. Compared to other LULC classes, the observed changes in this class were found to be minimal as also observed by Faisal et al. (2021), Kafy et al. (2022) and Gxokwe et al. (2023). Specifically, the water body exhibited an overall decrease from 2611.03 Km^2 to 2518.83 Km^2, resulting in a decline of 3.66 % between 1990 and 2020 (Figs. 9 and 10, and Table 6). The average ARC for this period was calculated at −0.12 % (Table 6), indicating a slight downward trend in water body coverage. During the period from 1990 to 2000, the water body experienced the highest decrease, with a reduction of 118.72 Km^2 (−4.55 %). This was followed by the period between 2000 and 2010, which had a decrease of 1.72 %. However, the period from 2010 to 2020 witnessed an increase in the water body, with a growth of 69.33 square kilometers (2.83 %) (Fig. 10 and Table 6).

Grassland change analysis

Between 1990 and 2020, there was a general decrease in the grassland area within the study area, from 25,014.52 Km^2 to 19,184.97 Km^2, representing a decline of 30.39 % (refer to Figs. 8 and 9, and Table 6). This form of trend was also observed by other studies (Kafy et al., 2022; Rahaman et al., 2022; Gxokwe et al., 2023). The average ARC for this period was calculated at −1.01 (Table 6), indicating a consistent downward trend in grassland coverage. The period from 2000 to 2010 exhibited the highest percentage decline in vegetation, with a decrease of approximately 20.56 %. This was followed by the period from 1990 to 2000, which recorded a decline of 5.38 % in the grassland area.

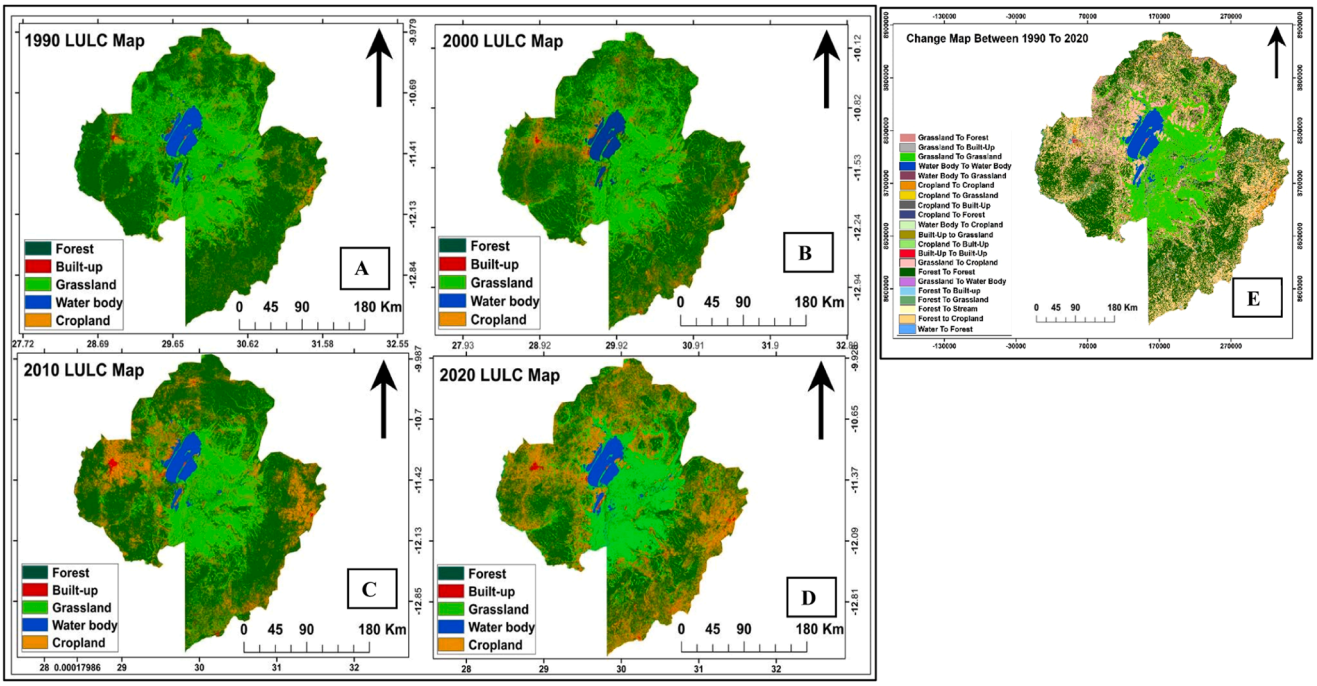

Fig. 7. Quad Hybrid Model classified maps of LULC for 1990 (A), 2000 (B), 2010 (C), 2020 (D), and 1990 to 2020 LULC change map (E).

Table 5
Estimates of LULC area and their percent coverage from 1990 to 2020.

Class Name	1990		2000		2010		2020	
	Area (km^2)	%	Area (km^2)	%	Area (km^2)	%	Area (km^2)	%
Forest	43,185.75	57.45	41,956.13	55.70	41,795.70	55.73	31,973.485	42.54
Built-up	428.89	0.571	603.27	0.80	707.44	0.94	873.29	1.16
Grassland	25,014.52	33.28	23,668.14	31.42	18,802.39	25.07	19,184.97	25.53
Water	2611.03	3.47	2492.31	3.31	2449.50	3.27	2518.83	3.35
Cropland	3925.11	5.22	6603.23	8.77	11,243.94	14.99	20,607.57	27.42

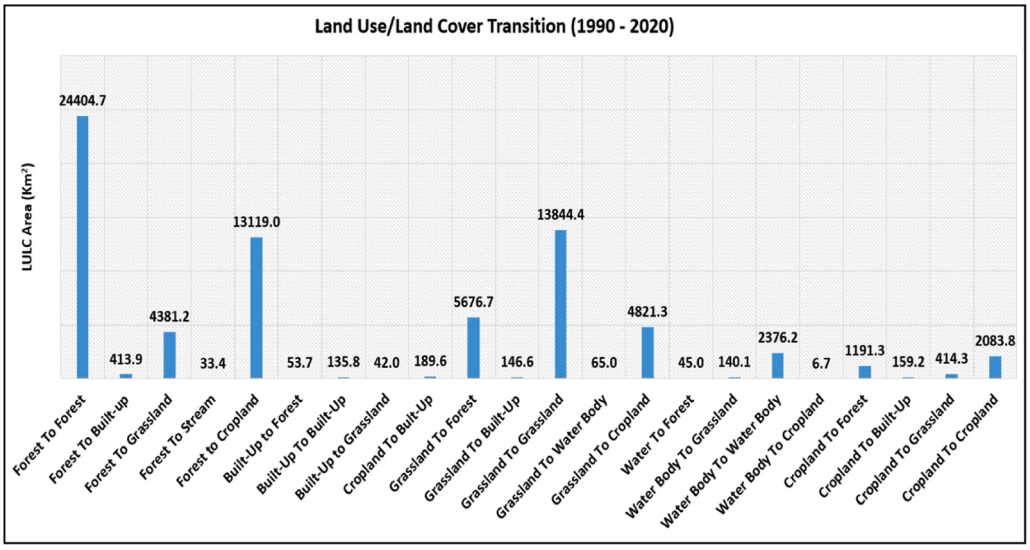

Fig. 8. The transition of LULC from one class to another class between 1990 and 2020 in the Bangweulu Wetland and its surrounding areas in Zambia.

However, the period between 2010 and 2020 showed a minimal increase in the grassland area, with a growth of 2.03 % (Fig. 9 and Table 6).

Table 6
Estimated percentage change in LULC from 1990 to 2020.

Class name	1990 - 2000		2000 - 2010		2010 - 2020		1990 - 2020		
	Area change (Km^2)	% Relative change	Area change (Km^2)	% Relative change	Area change (Km^2)	% Relative change	Area change (Km^2)	% Relative Change	% ARC
Forest Cover	−1229.62	−2.85	−160.43	−0.38	−9822.22	−23.50	−11,212.261	−35.07	−1.17
Built-up Area	174.38	40.659	104.18	17.27	165.84	23.44	444.40	50.89	1.70
Grassland	−1346.38	−5.38	−4865.75	−20.56	382.58	2.03	−5829.55	−30.39	−1.01
Water Body	−118.72	−4.55	−42.81	−1.72	69.33	2.83	−92.20	−3.66	−0.12
Cropland	2678.12	68.23	4640.72	70.28	9363.62	83.28	16,682.46	80.95	2.70

% Relative change is the difference between the LULC_end and the LULC_start divided by the LULC_start and multiplied by 100 {(LULC_end - LULC_start) / (LULC_start) * 100}.
%ARC: Percent Annual Rate of Change as described in Eq. (1) above. (% Relative Change/Time period).

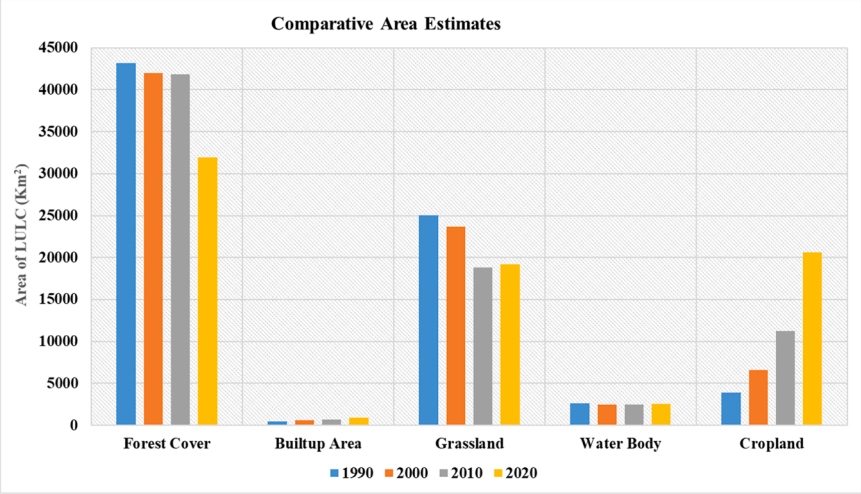

Fig. 9. Comparative area estimates for various LULC classes between 1990 and 2020.

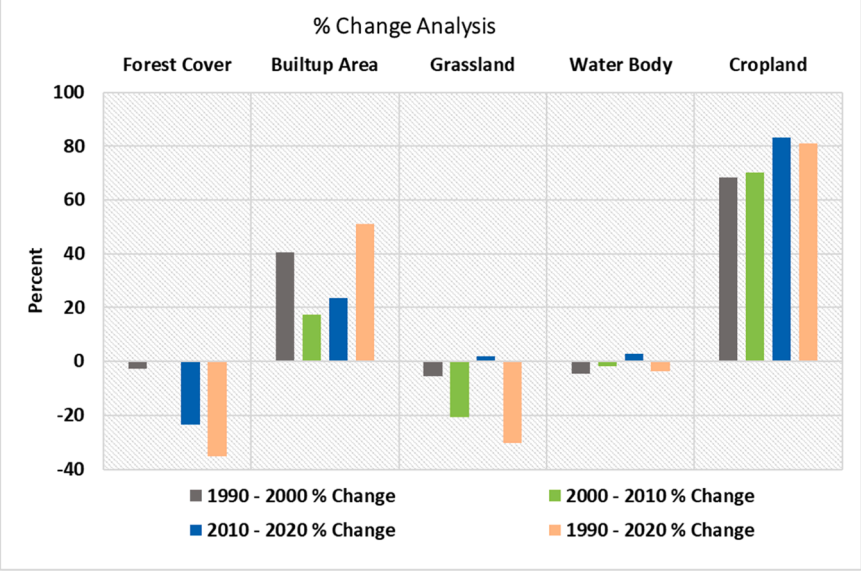

Fig. 10. Estimated percent change of different LULC classes between 1990 and 2020.

Discussion

Performance of different models

As earlier alluded to in Section 1, it's important to note that the performance of ML algorithms varies depending on the specific dataset, the complexity of the problem, the availability of data, sample size, methods, time and space. As the "No Free Lunch Theorem" suggests: there is no universal machine learning algorithm that performs best on all possible problems. This theorem highlights the fundamental limitations of ML algorithms in achieving optimal performance across all problem domains (Wolpert and Macready, 1997). Therefore, there are several reasons why the models in the study performed differently from one another as observed in Table 4. First of all, each machine learning method has its strengths and weaknesses. For example, some algorithms are better at handling complicated interactions and noisy data than others, which could be useful for specific LULC types (Adugna et al., 2022). Secondly, the models' performance might have been affected differently by the dimensionality, noise level, and class imbalance of the input data (Sun et al., 2009; Chao et al., 2022). Thirdly, there is a possibility that some algorithms were more successful for particular classes because different LULC classes typically exhibit different degrees of separability in the feature space (Abdi, 2020).

The RF model was excluded from further consideration as it did not meet the desired performance expectation (KI $>$ 0.6) for the classification of the 1990 and 2000 images as depicted in Fig. 5 above, indicating that it was a weaker model compared to DT, SVM, K-NN, and NB based on the methods used in this research. The RF is an ensemble model that utilises several decision trees as base classifiers, thus it was expected that it would outperform DT. However, in this study, DT performed better than RF which contradicts several studies (Gislason et al., 2006; Na et al., 2010; Kulkarni and Lowe, 2016). This was possible because this research used the minimum training sample size based on the previous literature.

DT can outperform the RF algorithm when the training sample size is limited due to its ability to create more flexible, simpler, and finer-grained decision boundaries which could potentially capture the specific patterns present in the limited data more effectively (Breiman, 2001b). Thakur & Panse (2022) also observed that it's easier to assess the performance of DT than RF with smaller data sets. Therefore, the underperformance of the RF model could potentially be attributed to the limited size of the training samples used in this research, assuming that the set parameters (Table 1 above) were optimal. In addition, the RF is an ensemble algorithm, which relies on the diversity and quality of weak learners (several decision trees), it typically benefits from larger and more diverse training data sets to create complex and stronger models, and this was also observed by Kulkarni & Lowe (2016) who stated that RF works well when provided with large homogeneous training data.

Thakur & Panse (2022) also added that RF requires a lot of resources and computational power as it relies on several decision trees for image classification. So, with the limited training sample size used in this research, the RF algorithm might have struggled to generalize well to unseen instances, as the limited training data set might not have adequately represented the full variability of the dataset, which could have restricted their ability to leverage the advantages of ensemble learning and the benefits of multiple models thereby creating an unstable decision tree with reduced accuracy (Caruana and Niculescu-Mizil, 2006; Polikar, 2006; Fernández-Delgado et al., 2014).

The KI and OA obtained from the four best performing models (SVM, NB, DT, and KNN) for the LULC classification of the BWS and the surrounding areas (Table 4) were reasonable based on Table 2 and consistent with several other studies (Tehrany et al., 2014; Basheer et al., 2022; Bayas et al., 2022). However, it is important to note that the performance of these four models exhibited differences in the values of the KI and OA. The two accuracy metrics (KI and OA) varied not only among the models but also with space and time (refer to Table 4). This could be attributed to atmospheric, surface, and illumination fluctuations, data sets, feature representation, hyperparameter adjustment, and the individual issue domain as observed by several other studies (Foody, 2008; Leyk et al., 2018; Rwanga and Ndambuki, 2017; Talukdar et al., 2020).

Hybrid machine learning

The fusion of the four models' maps (SVM, NB, DT, and KNN) produced the Quad hybrid maps with a higher KI and OA (Fig. 6 and Table 4) than any of the four models, showing that the Quad hybrid model's maps of the LULC were more accurate than any of the four models. This was expected because combining multiple models into a hybrid model allows for the creation of a more powerful and accurate model by leveraging the diverse strengths and weaknesses of different models as they capture distinct parts of the data and provide complementary predictions (Bagui, 2005; Polikar, 2006; Rokach, 2010; Chen et al., 2017). These results indicate that the Quad hybrid model could be an adaptable tool in enhancing the accuracy of modeling LULC changes for large-area mapping of wetlands, where there are limitations on resources and time coupled with challenges in gathering a large number of high-quality reference samples for calibration.

Land use/land cover trend analysis from 1990 to 2020 and policy implication

We employed the Quad hybrid model to understand the dynamic of the LULC of the Bangweulu Wetland and the surrounding area between 1990 and 2020. The trend analysis of LULC from 1990 to 2020 using the Quad hybrid model (Table 6 and Figs. 8, 9, 10, and 11) reveals several notable patterns as elaborated below.

There is a consistent decline in forest cover, water bodies, and grassland throughout the analysed period, this kind of trend was also observed by Muche et al. (2023). On the contrary, there is an upward trend in cropland and built-up areas the trend which was also observed by Gxokwe et al. (2023) and Taiwo et al. (2023). The decrease in the extent of forest cover and grassland could be mainly attributed to factors such as deforestation, urbanisation, and agricultural expansion, resulting in the conversion of natural land into agricultural fields and built-up infrastructure. The declining forest and grassland cover and increase in built-up and cropland areas in the BWS and the surrounding areas will have several impacts on both the wetland ecosystem itself and the surrounding environment. These impacts include (1) water quality deteriorations as observed by several other studies (Camara et al., 2019; Song et al., 2020; Tahiru et al., 2020; Nkwanda et al., 2021; Pandey et al., 2023;), (2) loss of biodiversity and habitat (Fenta et al., 2020; Perennou et al., 2020; Meng et al., 2023), (3) increased wetland sedimentation (Hernández-Romero et al., 2022), and (3) alterations in the microclimate such as variation of surface temperature (Kafy et al., 2021c, 2021a; AlDousari et al., 2023). In addition, the observed decrease in the surface water bodies, forest cover and grassland cover will accelerate the increasing patterns of drought severity in the BWS and the surrounding areas (Kafy et al., 2023).

There are various policy implications for the observed changes in LULC. A considerable environmental protection strategies are necessary to minimise deforestation and land degradation, given the fall in the forests and grassland covers. Policies for sustainable urban development are also required to deal with the significant rise in built-up areas which was also suggested by Dey et al. (2021) and Kafy et al. (2021b). The necessity for agricultural and food security measures, particularly the promotion of sustainable farming methods, is highlighted by the substantial growth of cropland. Furthermore, policies for managing water resources are necessary since the quantity of water in the open water bodies is decreasing.

In view of the above, the assessment of the water-body changes is critical for determining the natural and human-induced impact on the

water bodies. The continuous assessment of the changes in the water body could contribute knowledge to various fields, including studies on water resource management and disaster risk reduction, by providing critical information about the health and state of freshwater ecosystems (Sarp and Ozcelik, 2017; Wang et al., 2023). In addition, the long-term water-body change assessment and monitoring will be essential for evaluating the success of interventions, guiding conservation efforts, mitigating negative impacts on the wetland ecosystem, and determining whether the reduction in water in the BWS is a constant trend or a short-term phenomenon.

Limitations

The study has several limitations that should be considered. Firstly, it was difficult to distinguish certain wetland's different LULC features using 30-m Landsat images, which could lead to classification errors (Commey et al., 2023). Secondly, it could be possible that some of the models' hyper-parameters used might not have been fully optimised, which could affect how accurately the LULC maps were classified (Ebrahimi-Khusfi et al., 2021). Thirdly, the study used Landsat 5 images of 1990, 2000, and 2010, which had some sparkles in the 1990 and 2000 images, this could have led to poor performance in classifying certain LULC classes (Peng et al., 2023). In addition, this study used limited training sample size that might not have been adequately represented the full variability of the dataset. This could have restricted the ability of certain ML models such as the RF to generalise well to unseen instances thereby creating an unstable decision tree with reduced accuracy (Polikar, 2006; Fernández-Delgado et al., 2014). Lastly, the study excluded some models, such as the ANN model because it could not run in Orfeo Toolbox in QGIS 3.28.5, which might have limited the range of models considered for further analysis.

Conclusion

LULC change is a complex phenomenon that exerts profound effects on the environment, ecosystems, societies, and climate. Gaining an understanding of the impacts and implications of LULC change is crucial for implementing sustainable land management practices, conserving biodiversity, mitigating climate change, and fostering equitable and resilient societies.

The SVM, NB, DT, and KNN were identified as the best-performing ML models for the LULC classification in the Bangweulu Wetland and the surrounding areas. The Quad hybrid model was developed, which achieved a higher level of accuracy than individual ML models (SVM, NB, DT, and KNN). The developed Quad model was used to study the past and the present (1990 to 2020) LULC changes in the Bangweulu Wetland and the surrounding area.

The study has shown that there has been a consistent increase in cropland and built-up areas from 1990 to 2020 at the expense of the forest cover and grassland. The water body also experienced a gradual reduction between 1990 and 2020, although at a minimal rate.

Our observation highlights significant transformations in the LULC composition over the studied time frame. This could jeopardise the ecological integrity of the Bangweulu Wetland System, thereby compromising the provision of social, economic, and environmental benefits to both human and natural systems. It also highlights the need for effective land management strategies and sustainable planning to mitigate the potential impacts on natural ecosystems and ensure a balance between human activities and environmental conservation.

Recommendations

The following steps are proposed to validate the Quad hybrid model and the findings of the LULC changes;

- Evaluate the quad hybrid model's robustness: Use different periods, geographic locations, and data types to assess how consistently the Quad hybrid model performs.
- Examine the temporal and spatial patterns of changes in LULC: Identify areas of change hotspots, estimate rates and directions of change, and investigate the implications of these trends for ecosystem services such as water quality.
- Involve stakeholders and decision-makers: communicate the research results with interested parties, emphasise the value of sustainable land use and management, and compel the adoption of policies and practices that promote long-term social, economic, and environmental sustainability.

Ethical consideration

The University of Zambia Natural and Applied Sciences Research Ethics Committee approved this study.

Funding

This work was supported by mainly the O.R Tambo Africa Research Chair Initiative (ORTARChI) for water conservation project and partly by the African Union and the European Union under Wetlands Monitoring and Assessment (WeMAST) project and the Global Monitoring for Environment and Security (GMES) & Africa Support.

CRediT authorship contribution statement

Misheck Lesa Chundu: Writing – review & editing, Writing – original draft, Visualization, Validation, Software, Methodology, Investigation, Formal analysis, Data curation, Conceptualization. **Kawawa Banda:** Writing – review & editing, Supervision, Resources, Funding acquisition, Formal analysis. **Chisanga Lyoba:** Validation, Investigation, Data curation. **Greyfold Tembo:** Validation, Data curation. **Henry M. Sichingabula:** Supervision, Writing – review & editing. **Imasiku A. Nyambe:** Supervision, Writing – review & editing.

Declaration of competing interest

The authors do not have any conflicting interests (personal, financial, academic, or any other connections) to disclose that could potentially influence or bias the results, findings, or interpretations of this research.

Data availability

Data will be made available on request.

References

Abdi, A.M., 2020. Land cover and land use classification performance of machine learning algorithms in a boreal landscape using Sentinel-2 data. GISci. Remote Sens. 57 (1), 1–20. https://doi.org/10.1080/15481603.2019.1650447.

Abidi, S.M.R., Zhang, W., Haidery, S.A., Rizvi, S.S., Riaz, R., Ding, H., Kwon, S.J., 2020. Educational sustainability through big data assimilation to quantify academic procrastination using ensemble classifiers. Sustainability (Switzerland) 12 (15), 1–23. https://doi.org/10.3390/su12156074.

Adugna, T., Xu, W., Fan, J., 2022. Comparison of random forest and support vector machine classifiers for regional land cover mapping using coarse resolution FY-3C images. Remote Sens. (Basel) 14 (3), 1–22. https://doi.org/10.3390/rs14030574.

AlDousari, A.E., Kafy, A.Al, Saha, M., Fattah, M.A., Bakshi, A., Rahaman, Z.A., 2023. Summertime microscale assessment and prediction of urban thermal comfort zone using remote-sensing techniques for Kuwait. Earth. Syst. Environ. 7 (2), 435–456. https://doi.org/10.1007/s41748-023-00340-6.

Alshari, E.A., Gawali, B.W., 2022. Modeling land use change in Sana'a City of Yemen with MOLUSCE. J. Sens. 2022 https://doi.org/10.1155/2022/7419031.

Antunes, E., Vuppaladadiyam, A.K., Sarmah, A.K., Varsha, S.S.V., Pant, K.K., Tiwari, B., Pandey, A., 2021. Application of biochar for emerging contaminant mitigation. In:

Advances in Chemical Pollution, Environmental Management and Protection, 7. Elsevier, pp. 65–91. https://doi.org/10.1016/bs.apmp.2021.08.003.
Bagui, S.C., 2005. Combining pattern classifiers: methods and algorithms. In Technometrics (Vol. 47, Issue 4). 10.1198/tech.2005.s320.
Banda, A.M., Banda, K., Sakala, E., Chomba, M., Nyambe, I.A., 2023. Assessment of land use change in the wetland of Barotse Floodplain, Zambezi River Sub-Basin, Zambia. Nat. Hazards 115 (2), 1193–1211. https://doi.org/10.1007/s11069-022-05589-0.
Basheer, S., Wang, X., Farooque, A.A., Nawaz, R.A., Liu, K., Adekanmbi, T., Liu, S., 2022. Comparison of land use land cover classifiers using different satellite imagery and machine learning techniques. Remote Sens. (Basel) 14 (19), 1–18. https://doi.org/10.3390/rs14194978.
Bayas, S., Sawant, S., Dhondge, I., Kankal, P., Joshi, A., 2022. Land use land cover classification using different ML algorithms on sentinel-2 imagery. Lect. Notes Electr. Eng. 858, 761–777. https://doi.org/10.1007/978-981-19-0840-8_59.
Belgiu, M., Drăgu, L., 2016. Random forest in remote sensing: a review of applications and future directions. In: ISPRS Journal of Photogrammetry and Remote Sensing, 114. Elsevier, pp. 24–31. https://doi.org/10.1016/j.isprsjprs.2016.01.011.
Boateng, E.Y., Otoo, J., Abaye, D.A., 2020. Basic tenets of classification algorithms K-nearest-neighbor, support vector machine, random forest and neural network: a review. J. Data Anal. Inf. Process. 08 (04), 341–357. https://doi.org/10.4236/jdaip.2020.84020.
Breiman, L., 2001a. Statistical modeling: the two cultures. Stat. Sci. 16 (3), 199–215. https://doi.org/10.1214/ss/1009213726.
Breiman, L., 2001b. Random forests. Mach. Learn. 45 (1), 5–32. https://doi.org/10.1023/A:1010933404324/METRICS.
Camara, M., Jamil, N.R., Abdullah, A.F.Bin., 2019. Impact of land uses on water quality in Malaysia: a review. In: Ecological Processes, 8. Springer Verlag, pp. 1–10. https://doi.org/10.1186/s13717-019-0164-x.
Camargo, F.F., Sano, E.E., Almeida, C.M., Mura, J.C., Almeida, T., 2019. A comparative assessment of machine-learning techniques for land use and land cover classification of the Brazilian tropical savanna using ALOS-2/PALSAR-2 polarimetric images. Remote Sens. (Basel) 11 (13). https://doi.org/10.3390/rs11131600.
Caruana, R., Niculescu-Mizil, A., 2006. An empirical comparison of supervised learning algorithms. In: Proceedings of the ACM International Conference Proceeding Series, 148, pp. 161–168. https://doi.org/10.1145/1143844.1143865.
Chao, X., Kou, G., Peng, Y., Fernández, A., 2022. An efficiency curve for evaluating imbalanced classifiers considering intrinsic data characteristics: experimental analysis. Inf. Sci. (Ny) 608, 1131–1156. https://doi.org/10.1016/j.ins.2022.06.045.
Charif, O., Basse, R.M., Omrani, H., Trigano, P., 2012. Cellular automata model based on machine learning methods for simulating land use change. In: Proceedings of the Winter Simulation Conference, pp. 1846–1857. https://doi.org/10.1109/WSC.2012.6465098.
Chen, Y., Dou, P., Yang, X., 2017. Improving land use/cover classification with a multiple classifier system using AdaBoost integration technique. Remote Sensing 9 (10). https://doi.org/10.3390/rs9101055.
Chen, S., Webb, G.I., Liu, L., Ma, X., 2020. A novel selective naïve Bayes algorithm. Knowl. Based. Syst. 192, 105361 https://doi.org/10.1016/j.knosys.2019.105361.
Chollet, F., 2017. Machine learning. Mach. Learn. 45 (13), 40–48. https://doi.org/10.1007/978-1-4302-5990-9_1.
Commey, N.A., Magome, J., Ishidaira, H., Souma, K., 2023. Catchment-scale land use and land cover change analysis in two coastal ramsar sites in ghana, using remote sensing. Water (Switzerland) 15 (20), 1–21. https://doi.org/10.3390/w15203568.
Congalton, R.G., 2001. Accuracy assessment and validation of remotely sensed and other spatial information. Int. J. Wildland. Fire 10 (3–4), 321–328. https://doi.org/10.1071/wf01031.
Costanza, R., D'Arge, R., de Groot, R., Farber, S., Grasso, M., Hannon, B., Limburg, K., Naeem, S., O'Neill, R.V., Paruelo, J., Raskin, R.G., Sutton, P., & van den Belt, M., 1997. The value of the world's ecosystem services and natural capital. LK - https://royalroads.on.worldcat.org/oclc/4592801201. Nature TA - TT -, 387(6630), 253–260.
Cutler, A., Cutler, D.R., Stevens, J.R., 2012. Ensemble machine learning. Ensemble Mach. Learn. https://doi.org/10.1007/978-1-4419-9326-7. February 2014.
Dalianis, H., 2018. Evaluation metrics and evaluation. In Clinical Text Mining (Issue 1967, pp. 45–53). 10.1007/978-3-319-78503-5_6.
Davidson, N.C., 2014. How much wetland has the world lost? Long-term and recent trends in global wetland area. Mar. Freshw. Res. 65 (10), 934–941. https://doi.org/10.1071/MF14173.
De Araujo Barbosa, C.C., Atkinson, P.M., Dearing, J.A., 2015. Remote sensing of ecosystem services: a systematic review. Ecol. Indic. 52, 430–443. https://doi.org/10.1016/j.ecolind.2015.01.007.
Dey, N.N., Al Rakib, A., Kafy, A.Al, Raikwar, V., 2021. Geospatial modelling of changes in land use/land cover dynamics using Multi-layer perception Markov chain model in Rajshahi City, Bangladesh. Environ. Challenges 4 (March), 100148. https://doi.org/10.1016/j.envc.2021.100148.
Ebrahimi-Khusfi, Z., Nafarzadegan, A.R., Dargahian, F., 2021. Predicting the number of dusty days around the desert wetlands in southeastern Iran using feature selection and machine learning techniques. Ecol. Indic. 125 (February), 107499 https://doi.org/10.1016/j.ecolind.2021.107499.
Etikan, I., 2016. Comparison of convenience sampling and purposive sampling. Am. J. Theor. Appl. Stat. 5 (1), 1. https://doi.org/10.11648/j.ajtas.20160501.11.
Faisal, A.Al, Kafy, A.A., Al Rakib, A., Akter, K.S., Jahir, D.M.A., Sikdar, M.S., Ashrafi, T. J., Mallik, S., Rahman, M.M., 2021. Assessing and predicting land use/land cover, land surface temperature and urban thermal field variance index using Landsat imagery for Dhaka Metropolitan area. Environ. Challenges 4 (April), 100192. https://doi.org/10.1016/j.envc.2021.100192.
Fanshawe, D., 1971. The vegetation of Zambia, Printed by the Government Printer. https://www.worldcat.org/title/vegetation-of-zambia/oclc/1323510.
FAO, 2017. Water Pollution from Agriculture: A Global Review. The Food and Agricultural Organisation, pp. 1–35. https://www.fao.org/3/i7754e/i7754e.pdf.
Fenta, A.A., Tsunekawa, A., Haregeweyn, N., Tsubo, M., Yasuda, H., Shimizu, K., Kawai, T., Ebabu, K., Berihun, M.L., Sultan, D., Belay, A.S., Sun, J., 2020. Cropland expansion outweighs the monetary effect of declining natural vegetation on ecosystem services in sub-Saharan Africa. Ecosyst. Serv. 45 (April), 101154 https://doi.org/10.1016/j.ecoser.2020.101154.
Fernández-Delgado, M., Cernadas, E., Barro, S., Amorim, D., 2014. Do we need hundreds of classifiers to solve real world classification problems? J. Mach. Learn. Res. 15 (April 2020), 3133–3181. https://doi.org/10.1117/1.JRS.11.015020.
Foody, G., 2008. Harshness in image classification accuracy assessment. Int. J. Remote Sens. 29 (11), 3137–3158. https://doi.org/10.1080/01431160701442120.
Galatowitsch, S.M., 2018. Natural and anthropogenic drivers of wetland change. In: The Wetland Book II: Distribution, Description, and Conservation, 1. Springer, Dordrecht, pp. 359–367. https://doi.org/10.1007/978-94-007-4001-3_217.
Gholami, R., Fakhari, N., 2017. Support vector machine: principles, parameters, and applications. Handbook of Neural Computation. Elsevier Inc, pp. 515–535. https://doi.org/10.1016/B978-0-12-811318-9.00027-2.
Gislason, P.O., Benediktsson, J.A., Sveinsson, J.R., 2006. Random Forests for land cover classification. Pattern. Recognit. Lett. 27 (4), 294–300. https://doi.org/10.1016/J.PATREC.2005.08.011.
Guan, H., Li, J., Chapman, M., Deng, F., Ji, Z., Yang, X., 2013. Integration of orthoimagery and lidar data for object-based urban thematic mapping using random forests. Int. J. Remote Sens. 34 (14), 5166–5186. https://doi.org/10.1080/01431161.2013.788261.
Gxokwe, S., Dube, T., Mazvimavi, D., 2023. An assessment of long-term and large-scale wetlands change dynamics in the Limpopo transboundary river basin using cloud-based Earth observation data. Wetl. Ecol. Manage. https://doi.org/10.1007/s11273-023-09963-y, 0123456789.
Hayes, M.M., Miller, S.N., Murphy, M.A., 2014. High-resolution landcover classification using random forest. Remote Sens. Lett. 5 (2), 112–121. https://doi.org/10.1080/2150704X.2014.882526.
Hemati, M., Hasanlou, M., Mahdianpari, M., Mohammadimanesh, F., 2021. A systematic review of landsat data for change detection applications: 50 years of monitoring the earth. Remote Sens. (Basel) 13 (15). https://doi.org/10.3390/rs13152869.
Hernández-Romero, G., Álvarez-Martínez, J.M., Pérez-Silos, I., Silió-Calzada, A., Vieites, D.R., Barquín, J., 2022. From forest dynamics to wetland siltation in mountainous landscapes: a RS-based framework for enhancing erosion control. Remote Sens. (Basel) 14 (8). https://doi.org/10.3390/rs14081864.
Hernandez, I., Benevides, P., Costa, H., Caetano, M., 2020. Exploring sentinel-2 for land cover and crop mapping in portugal. In: Proceedings of the International Archives of the Photogrammetry, Remote Sensing and Spatial Information Sciences - ISPRS Archives, 43, pp. 83–89. https://doi.org/10.5194/isprs-archives-XLIII-B3-2020-83-2020.
Hosseiny, B., Abdi, A.M., Jamali, S., 2022. Urban land use and land cover classification with interpretable machine learning – A case study using Sentinel-2 and auxiliary data. Remote Sens. Appl. Soc. Environ. 28 (September), 100843 https://doi.org/10.1016/j.rsase.2022.100843.
Huntington, J.L., Hegewisch, K.C., Daudert, B., Morton, C.G., Abatzoglou, J.T., McEvoy, D.J., Erickson, T., 2017. Climate engine: cloud computing and visualization of climate and remote sensing data for advanced natural resource monitoring and process understanding. Bull. Am. Meteorol. Soc. 98 (11), 2397–2409. https://doi.org/10.1175/BAMS-D-15-00324.1.
Kafy, A.Al, Rahman, M.S., Faisal, A.Al, Hasan, M.M., Islam, M., 2020. Modelling future land use land cover changes and their impacts on land surface temperatures in Rajshahi, Bangladesh. Remote Sens. Appl. Soc. Environ. 18 https://doi.org/10.1016/j.rsase.2020.100314.
Kafy, A.Al, Faisal, A.Al, Shuvo, R.M., Naim, M.N.H., Sikdar, M.S., Chowdhury, R.R., Islam, M.A., Sarker, M.H.S., Khan, M.H.H., Kona, M.A., 2021a. Remote sensing approach to simulate the land use/land cover and seasonal land surface temperature change using machine learning algorithms in a fastest-growing megacity of Bangladesh. Remote Sens. Appl. Soc. Environ. 21 https://doi.org/10.1016/j.rsase.2020.100463.
Kafy, A.A., Naim, M.N.H., Subramanyam, G., Faisal, A.Al, Ahmed, N.U., Rakib, A.Al, Kona, M.A., Sattar, G.S., 2021b. Cellular Automata approach in dynamic modelling of land cover changes using RapidEye images in Dhaka, Bangladesh. Environ. Challenges 4 (March), 100084. https://doi.org/10.1016/j.envc.2021.100084.
Kafy, A.Al, Dey, N.N., Al Rakib, A., Rahaman, Z.A., Nasher, N.M.R., Bhatt, A, 2021c. Modeling the relationship between land use/land cover and land surface temperature in Dhaka, Bangladesh using CA-ANN algorithm. Environ. Challenges 4 (May), 100190. https://doi.org/10.1016/j.envc.2021.100190.
Kafy, A.Al., Saha, M., Faisal, A.Al., Rahaman, Z.A., Rahman, M.T., Liu, D., Fattah, M.A., Al Rakib, A., AlDousari, A.E., Rahaman, S.N., Hasan, M.Z., Ahasan, M.A.K., 2022. Predicting the impacts of land use/land cover changes on seasonal urban thermal characteristics using machine learning algorithms. Building and Environment 217, 109066. https://doi.org/10.1016/j.buildenv.2022.109066.
Kafy, A.Al, Bakshi, A., Saha, M., Faisal, A.Al, Almulhim, A.I., Rahaman, Z.A., Mohammad, P, 2023. Assessment and prediction of index based agricultural drought vulnerability using machine learning algorithms. Sci. Total Environ. 867 https://doi.org/10.1016/j.scitotenv.2023.161394.
Kamweneshe, B., Beilfuss, R., & Morrison, K., 2003. Population and distribution of Wattled Cranes and other large waterbirds and large mammals on the Liuwa Plains National Park, Zambia. 10.13140/RG.2.2.26628.32647.

Kang, H.Y., Rule, R.A., Noble, P.A., 2012. Artificial neural network modeling of phytoplankton blooms and its application to sampling sites within the same estuary. In: Treatise on Estuarine and Coastal Science, 9. Elsevier Inc, pp. 161–172. https://doi.org/10.1016/B978-0-12-374711-2.00908-6.

Kulkarni, A.D., Lowe, B., 2016. Random forest algorithm for land cover classification. Int. J. Recent Innov. Trends Comput. Commun. 4 (3), 58. –. http://hdl.handle.net/10950/341.

Kumar, A., Kanaujia, A., 2018. Wetlands: significance, threats and their conservation. Envis Center 7 (March 2014), 3&4. https://www.researchgate.net/publication/327816889.

Laban, N., Abdellatif, B., Ebeid, H.M., Shedeed, H.A., Tolba, M.F., 2019. Machine learning for enhancement land cover and crop types classification. Stud. Comput. Intell. 801 (April), 71–87. https://doi.org/10.1007/978-3-030-02357-7_4.

Landis, J.R., Koch, G.G., 1977. The measurement of observer agreement for categorical data. Biometrics 33 (1), 159. https://doi.org/10.2307/2529310.

Lasanta, T., Vicente-Serrano, S.M., 2012. Complex land cover change processes in semiarid Mediterranean regions: an approach using Landsat images in northeast Spain. Remote Sens. Environ. 124, 1–14. https://doi.org/10.1016/j.rse.2012.04.023.

Lehner, B., Katiyo, L., Chivava, F., Sichingabula, H.M., Nyirenda, E., Rivers-Moore, N.A., Paxton, B.R., Grill, G., Nyoni, F., Shamboko-Mbale, B., Banda, K., Thieme, M.L., Silembo, O.M., Musutu, A., Filgueiras, R., 2021. Identifying priority areas for surface water protection in data scarce regions: an integrated spatial analysis for Zambia. Aquat. Conserv. Mar. Freshw. Ecosyst. 31 (8), 1998–2016. https://doi.org/10.1002/aqc.3606.

Leyk, S., Uhl, J.H., Balk, D., Jones, B., 2018. Assessing the accuracy of multi-temporal built-up land layers across rural-urban trajectories in the United States. Remote Sens. Environ. 204, 898–917. https://doi.org/10.1016/J.RSE.2017.08.035.

Loussaief, S., Abdelkrim, A., 2017. Machine learning framework for image classification. In: Proceedings of the 7th International Conference on Sciences of Electronics, Technologies of Information and Telecommunications, 3, pp. 58–61. https://doi.org/10.1109/SETIT.2016.7939841. SETIT 2016.

Lu, D., Mausel, P., Brondízio, E., Moran, E., 2004. Change detection techniques. Int. J. Remote Sens. 25 (12), 2365–2401. https://doi.org/10.1080/0143116031000139863.

Ma, L., Li, M., Ma, X., Cheng, L., Du, P., Liu, Y., 2017. A review of supervised object-based land-cover image classification. In: ISPRS J. Photogramm. Remote Sens., 130. Elsevier, pp. 277–293. https://doi.org/10.1016/j.isprsjprs.2017.06.001.

Mahmoud, R., Hassanin, M., Al Feel, H., Badry, R.M., 2023. Machine learning-based land use and land cover mapping using multi-spectral satellite imagery: a case study in Egypt. Sustainability (Switzerland) 15 (12), 1–21. https://doi.org/10.3390/su15129467.

Maitima, J., Olson, J., Mugatha, S., Mugisha, S., Mutie, I., 2010. Land use changes, impacts and options for sustaining productivity and livelihoods in the basin of lake Victoria. J. Sustain. Dev. Afr. https://www.researchgate.net/publication/257657203_Land_use_changes_impacts_and_options_for_sustaining_productivity_and_livelihoods_in_the_basin_of_lake_Victoria.

Maxwell, A.E., Warner, T.A., Fang, F., 2018. Implementation of machine-learning classification in remote sensing: an applied review. Int. J. Remote Sens. 39 (9), 2784–2817. https://doi.org/10.1080/01431161.2018.1433343.

McHugh, M.L., 2012. Interrater reliability: the kappa statistic. Biochem. Med. (Zagreb) 22 (3), 276–282. https://doi.org/10.11613/bm.2012.031.

Meng, Z., Dong, J., Ellis, E.C., Metternicht, G., Qin, Y., Song, X.P., Löfqvist, S., Garrett, R. D., Jia, X., Xiao, X., 2023. Post-2020 biodiversity framework challenged by cropland expansion in protected areas. Nat. Sustain. https://doi.org/10.1038/s41893-023-01093-w.

Mohammadpour, P., Viegas, D.X., Viegas, C., 2022. Vegetation mapping with random forest using sentinel 2 and GLCM texture feature—a case study for Lousã Region, Portugal. Remote Sens. (Basel) 14 (18). https://doi.org/10.3390/rs14184585.

Moraes, D., Benevides, P., Costa, H., Moreira, F.D., Caetano, M., 2021. Influence of sample size in land cover classification accuracy using random forest and sentinel-2 data in Portugal. Int. Geosci. Remote Sens. Symp. (IGARSS) 4232–4235. https://doi.org/10.1109/IGARSS47720.2021.9553924.

Muche, M., Yemata, G., Molla, E., Adnew, W., Muasya, A.M., 2023. Land use and land cover changes and their impact on ecosystem service values in the north-eastern highlands of Ethiopia. PLoS One 18 (9 September). https://doi.org/10.1371/journal.pone.0289962.

Na, X., Zhang, S., Li, X., Yu, H., Liu, C., 2010. Improved land cover mapping using random forests combined with Landsat thematic mapper imagery and ancillary geographic data. Photogramm. Eng. Remote Sens. 76 (7), 833–840. https://doi.org/10.14358/PERS.76.7.833.

Ngoma, H., Hamududu, B.H., Resources, N.W., Directorate, E., Hangoma, P., & Samboko, P.C., 2017. Irrigation development for climate resilience in Zambia: the known knowns and known unknowns. In Research gate (Issue January 2018). https://www.canr.msu.edu/resources/irrigation-development-for-climate-resilience-in-zambia-the-known-knowns-and-known-unknowns.

Nkwanda, I.S., Feyisa, G.L., Zewge, F., Makwinja, R., 2021. Impact of land-use/land-cover dynamics on water quality in the Upper Lilongwe River basin, Malawi. Int. J. Energy Water Resourc. 5 (2), 193–204. https://doi.org/10.1007/s42108-021-00125-5.

Ouma, Y., Nkwae, B., Moalafhi, D., Odirile, P., Parida, B., Anderson, G., Qi, J., 2022. Comparison of machine learning classifiers for multitemporal and multisensor mapping of urban LULC features. International archives of the photogrammetry. Remote Sens. Spat. Inf. Sci. - ISPRS Arch. 43 (B3–2022), 681–689. https://doi.org/10.5194/isprs-archives-XLIII-B3-2022-681-2022.

Pandey, S., Kumari, N., Al Nawajish, S., 2023. Land Use Land Cover (LULC) and surface water quality assessment in and around Selected Dams of Jharkhand using Water Quality Index (WQI) and Geographic Information System (GIS). J. Geol. Soc. India 99 (2), 205–218. https://doi.org/10.1007/s12594-023-2288-y.

Peng, K., Jiang, W., Hou, P., Wu, Z., Cui, T., 2023. Detailed wetland-type classification using Landsat-8 time-series images: a pixel- and object-based algorithm with knowledge (POK). GIsci. Remote Sens. 61 (1) https://doi.org/10.1080/15481603.2023.2293525.

Perennou, C., Gaget, E., Galewski, T., Geijzendorffer, I., Guelmami, A., 2020. Evolution of wetlands in Mediterranean region. Water Resourc. Mediterranean Region 297–320. https://doi.org/10.1016/B978-0-12-818086-0.00011-X.

Polikar, R., 2006. Ensemble based systems in decision making. In: Proceedings of the IEEE Circuits and Systems Magazine, 6, pp. 21–44. https://doi.org/10.1109/MCAS.2006.1688199.

Qiu, C., Jiang, L., Li, C., 2015. Not always simple classification: learning SuperParent for class probability estimation. Expert. Syst. Appl. 42 (13), 5433–5440. https://doi.org/10.1016/j.eswa.2015.02.049.

Rahaman, Z.A., Kafy, A.Al, Saha, M., Rahim, A.A., Almulhim, A.I., Rahaman, S.N., Fattah, M.A., Rahman, M.T., S, K., Faisal, A.Al, Al Rakib, A., 2022. Assessing the impacts of vegetation cover loss on surface temperature, urban heat island and carbon emission in Penang city, Malaysia. Build. Environ. 222, 109335 https://doi.org/10.1016/j.buildenv.2022.109335.

Ramezan, C.A., Warner, T.A., Maxwell, A.E., Price, B.S., 2021. Effects of training set size on supervised machine-learning land-cover classification of large-area high-resolution remotely sensed data. Remote Sens. (Basel) 13 (3), 1–27. https://doi.org/10.3390/rs13030368.

Ramsar Convention on Wetlands., 2018. Global wetland outlook: state of the world's wetlands and their services to people. https://www.researchgate.net/publication/328093181_Global_Wetland_Outlook_State_of_the_World's_Wetlands_and_Their_Services_to_People.

Ren, J.P., Wang, J., Gu, A.L., Zuo, L.B., Sun, H.W., Xu, K.K., He, F.Q., Mukofu, C., Dokowe, A.P., & Chikambwe, E., 2021. Gold enrichment characteristics and exploration prospects in Zambia: based on 1:1000000 geochemical mapping. 10.1016/S2096-5192(22)00086-6.

Rokach, L., 2010. Ensemble-based classifiers. Artif. Intell. Rev. 33 (1–2), 1–39. https://doi.org/10.1007/s10462-009-9124-7.

Rwanga, S.S., Ndambuki, J.M., 2017. Accuracy assessment of land use/land cover classification using remote sensing and GIS. Int. J. Geosci. 08 (04), 611–622. https://doi.org/10.4236/ijg.2017.84033.

Sadiq, R., Rodriguez, M.J., Mian, H.R., 2019. Empirical models to predict disinfection by-products (DBPs) in drinking water: an updated review. Encyclopedia of Environmental Health. Elsevier, pp. 324–338. https://doi.org/10.1016/B978-0-12-409548-9.11193-5.

Sarp, G., Ozcelik, M., 2017. Water body extraction and change detection using time series: a case study of Lake Burdur, Turkey. J. Taibah Univ. Sci. 11 (3), 381–391. https://doi.org/10.1016/j.jtusci.2016.04.005.

Simaika, J.P., Chakona, A., van Dam, A.A., 2021. Editorial: towards the sustainable use of African Wetlands. Front. Environ. Sci. 9 (March), 1–4. https://doi.org/10.3389/fenvs.2021.658871.

Song, Y., Song, X., Shao, G., Hu, T., 2020. Effects of land use on stream water quality in the rapidly urbanized areas: a multiscale analysis. Water (Switzerland) 12 (4). https://doi.org/10.3390/W12041123.

Storrs, J., 1995. Know your trees: some of the common trees found in Zambia. Regional Soil Conservation Unit, (RSCU). Regional Soil Conservation Unit. https://www.worldcat.org/title/know-your-trees-some-of-the-common-trees-found-in-zambia/oclc/7979762/editions?referer=di&editionsView=true.

Sun, Y., Wong, A.K.C., Kamel, M.S., 2009. Classification of imbalanced data: a review. Intern. J. Pattern. Recognit. Artif. Intell. 23 (4), 687–719. https://doi.org/10.1142/S0218001409007326.

Tahiru, A.A., Doke, D.A., Baatuuwie, B.N., 2020. Effect of land use and land cover changes on water quality in the Nawuni Catchment of the White Volta Basin, Northern Region, Ghana. Appl. Water. Sci. 10 (8), 1–14. https://doi.org/10.1007/s13201-020-01272-6.

Taiwo, B.E., Kafy, A.Al, Samuel, A.A., Rahaman, Z.A., Ayowole, O.E., Shahrier, M., Duti, B.M., Rahman, M.T., Peter, O.T., Abosede, O.O., 2023. Monitoring and predicting the influences of land use/land cover change on cropland characteristics and drought severity using remote sensing techniques. Environ. Sustain. Indicat. 18 (March), 100248 https://doi.org/10.1016/j.indic.2023.100248.

Talukdar, S., Singha, P., Mahato, S., & Pal, S., 2020. Land-use land-cover classification by machine learning classifiers for satellite observations — a review. 10.3390/rs12071135.

Tehrany, M.S., Pradhan, B., Jebuv, M.N., 2014. A comparative assessment between object and pixel-based classification approaches for land use/land cover mapping using SPOT 5 imagery. Geocarto Int. 29 (4), 351–369. https://doi.org/10.1080/10106049.2013.768300.

Thakur, R., Panse, P., 2022. Classification Performance of Land Use from Multispectral Remote Sensing Images using Decision Tree, K-Nearest Neighbor, Random Forest and Support Vector Machine Using EuroSAT Data. Int. J. Intell. Syst. Appl. Eng. 10, 67–77 (1s). https://ijisae.org/index.php/IJISAE/article/view/2238.

Thamaga, K.H., Dube, T., Shoko, C., 2022. Evaluating the impact of land use and land cover change on unprotected wetland ecosystems in the arid-tropical areas of South Africa using the Landsat dataset and support vector machine. Geocarto Int. 37 (25), 10344–10365. https://doi.org/10.1080/10106049.2022.2034986.

Wambugu, N., Chen, Y., Xiao, Z., Wei, M., Aminu Bello, S., Marcato Junior, J., Li, J., 2021. A hybrid deep convolutional neural network for accurate land cover

classification. Int. J. Appl. Earth Observ. Geoinf. 103 https://doi.org/10.1016/j.jag.2021.102515.

Wang, W., Teng, H., Zhao, L., Han, L., 2023. Long-term changes in water body area dynamic and driving factors in the middle-lower yangtze plain based on multi-source remote sensing data. Remote Sens. 15 (7), 1816. https://doi.org/10.3390/rs15071816.

Winton, R.S., Teodoru, C.R., Calamita, E., Kleinschroth, F., Banda, K., Nyambe, I., Wehrli, B., Winton, R.S., 2021. Anthropogenic influences on Zambian water quality: hydropower and land-use change. Environ. Sci. 23 (7), 981–994. https://doi.org/10.1039/d1em00006c processes and Impacts.

Wolpert, D.H., Macready, W.G., 1997. No free lunch theorems for optimization. IEEE Trans. Evol. Comp. 1 (1), 67–82. https://doi.org/10.1109/4235.585893.

Wulder, M.A., Loveland, T.R., Roy, D.P., Crawford, C.J., Masek, J.G., Woodcock, C.E., Allen, R.G., Anderson, M.C., Belward, A.S., Cohen, W.B., Dwyer, J., Erb, A., Gao, F., Griffiths, P., Helder, D., Hermosilla, T., Hipple, J.D., Hostert, P., Hughes, M.J., Zhu, Z., 2019. Current status of Landsat program, science, and applications. Remote Sens. Environ. 225, 127–147. https://doi.org/10.1016/j.rse.2019.02.015.

Xu, T., Weng, B., Yan, D., Wang, K., Li, X., Bi, W., Li, M., Cheng, X., Liu, Y., 2019. Wetlands of international importance: status, threats, and future protection. Int. J. Environ. Res. Public Health 16 (10). https://doi.org/10.3390/ijerph16101818.

Yuh, Y.G., Tracz, W., Matthews, H.D., Turner, S.E., 2023. Application of machine learning approaches for land cover monitoring in northern Cameroon. Ecol. Inform. 74 (December 2022), 101955 https://doi.org/10.1016/j.ecoinf.2022.101955.

Zambia Environment Outlook Report 4., 2017. www.zema.org.zm:https://ISBN:9789982705981.

Zambia Wildlife Authority., 2006. Information Sheet on Ramsar Wetlands (RIS)–2006-2008 version (Vol. 7, Issue 1990). https://rsis.ramsar.org/RISapp/files/RISrep/ZM531RIS.pdf.

Zedler, J.B., Kercher, S., 2005. Wetland resources: status, trends, ecosystem services, and restorability. Annu Rev. Environ. Resour. 30, 39–74. https://doi.org/10.1146/annurev.energy.30.050504.144248.

Zhang, M., Zhang, C., Kafy, A.Al, Tan, S., 2021. Simulating the relationship between land use/cover change and urban thermal environment using machine learning algorithms in Wuhan City, China. Land. (Basel) 11 (1), 14. https://doi.org/10.3390/LAND11010014, 2022.